EL SEVIER

Contents lists available at ScienceDirect

# **Surface & Coatings Technology**

journal homepage: www.elsevier.com/locate/surfcoat



# Deposition and characterization of a ZrN/Zr/a-C multilayer: Implication on bio-tribological and corrosion behaviors



W.Q. Bai a, L.L. Li a,b, R.L. Li b, C.D. Gu a, X.L. Wang a, G. Jin b, D.G. Liu c, J.P. Tu a,\*

- <sup>a</sup> State Key Laboratory of Silicon Materials, School of Materials Science and Engineering, Zhejiang University, Hangzhou 310027, China
- <sup>b</sup> Zhongao Huicheng Technology Co. Ltd., Beijing 100176, China
- <sup>c</sup> No.38 Research Institute of CETC., Hefei 230088, China

#### ARTICLE INFO

Article history: Received 17 November 2016 Revised 7 April 2017 Accepted in revised form 22 May 2017 Available online 23 May 2017

Keywords: Amorphous carbon ZrN Multilayer Bio-tribological performance Corrosion resistance

#### ABSTRACT

The ZrN/Zr/a-C multilayered coatings were deposited onto Ti6Al4V and Si substrates using a closed field unbalanced magnetron sputtering. The morphology and microstructure of the multilayers were performed by scanning electron microscopy (SEM), atomic force microscopy (AFM) and transmission electron microscopy (TEM). The multilayer consists of a-C layers, Zr layers and ZrN layers. The Zr interlayers can improve the weak adhesion between a-C layers and ZrN layers. The multilayer exhibits a low residual stress of -0.5 GPa and a hardness of 18.7 GPa. The tribological properties were evaluated by a ball-on-disk tribometer. The friction coefficient and wear rate of the multilayer in fetal bovine serum (FBS) kept very low values during sliding at an applied load of 2 N, which indicated excellent long-term wear resistance. What is more, the multilayer also presented a low wear rate in FBS even at a high applied load of 10 N. Additionally, the corrosion resistance of Ti6Al4V in Hank's solution is significantly improved by the multilayer. This study demonstrates that the ZrN/Zr/a-C multilayer exhibits excellent performance including low residual stress, high corrosion resistance as well as good bio-tribological properties and it is proper to protect Ti6Al4V alloy.

© 2017 Elsevier B.V. All rights reserved.

## 1. Introduction

Hip and knee artificial joints are designed to retain mobility and reduce the pain, which have been ubiquitously used in surgical operations [1]. The amount of hip and knee replacements has been increased significantly by a percentage of 15–22% worldwide within the last five years [2]. Another noteworthy issue is that the amount of younger patients requiring joint replacement is increasing, which generate the demand of longer service life for hip and knee artificial joints [3].

Ti6Al4V alloy is widely used in the stem of an artificial hip joint. However, the stem is assembled with a chromium-cobalt alloy head through taper joints due to the low wear resistance of Ti6Al4V. Although the chromium-cobalt alloy shows high wear and corrosion resistance, the taper joint becomes a key source of wear debris, which can lead to aseptic loosening. A hard coating such as a-C can be deposited onto Ti6Al4V and improve its tribological behavior, which makes the design (a single part of "stem and head using Ti6Al4V alloy") promising [2]. Some certain outstanding advantages such as high hardness, high wear and corrosion resistance, superior biocompatibility and good chemical inertness have kept driving the working force to be contributed into a-C coating in the past two decades [4–8]. Unfortunately, the

major drawbacks of high residual stress and low adhesion to metallic substrate hinder its application [9,10]. In order to overcome the drawbacks of a-C coating, the interlayered and multilayered structures are introduced [11-18]. Leyland and Matthews suggest that the coatings with multilayered structure (a softer layer placed between two harder layers) exhibit improved toughness and may arrest crack propagation at the internal interfaces by energy dissipation and crack deflection [19].The interlayers such as Ti. Cr and their carbides or nitrides are known to reduce the residual stress of coating and therefore improve the adhesion of the coating to substrate [20-22]. Multilayered a-C coatings are highly appropriate for use in orthopedics implants due to their higher resistance to cohesive and adhesive crack propagation compared to single layered coating [2,23,24]. Recently, Major et al. and Kot et al. reported a new type of TiN/Ti/a-C: H multilayered coatings, which exhibited good mechanical properties and high biocompatibility, but the tribological performances and corrosion behaviors of them were still not fully understood [25,26]. Additionally, Pejaković et al. shows that Zr-based nitride coatings present a superior friction and wear behavior compared to Ti-based coatings in Na<sub>2</sub>SO<sub>4</sub> solution, which suggests that ZrN is more appropriate than TiN to be introduced into a-C multilayer

Consequently, in this present work, a ZrN/Zr/a-C multilayer is fabricated by an industrial closed field unbalanced magnetron sputtering. The tribological performance of the coating has been studied in detail

<sup>\*</sup> Corresponding author.

E-mail addresses: tujp@zju.edu.cn, tujplab@zju.edu.cn (J.P. Tu).

in a presence of FBS. The corrosion behavior is also investigated in simulated body fluid (Hank's solution).

### 2. Materials and methods

A closed field unbalanced magnetron sputtering equipped with high purity zirconium (99.9%) and graphite (99.9%) targets was used for coating deposition. Before deposition, a base pressure of  $3 \times 10^{-3}$  Pa in the chamber was attained. During the deposition, the temperature was set to 100 °C. A negative bias pulse with a frequency of 60 kHz and a duty cycle of 35% was employed to provide substrate bias. The Ti6Al4V and Si substrates were employed in this work. The coatings deposited on Si substrates were used to characterize the microstructure and hardness, while those on Ti6Al4V substrates were employed to evaluate the wear and corrosion behaviors. For the multilayered coating, first a Zr interlayer was deposited onto the substrates in order to improve the adhesion strength. Then the multilayer were produced by the sequence of a-C, Zr, ZrN and Zr layer. The top layer is a-C layer. The a-C and Zr layers were deposited in an argon atmosphere, while for the deposition of ZrN layers the nitrogen was introduced into the chamber. For comparison, a-C and ZrN coatings were also prepared. The thickness of ZrN/Zr/a-C, ZrN and a-C coating is about 2.3 μm, 1.3 μm and 1.0 μm respectively.

The phase analysis were performed with X-ray diffraction (XRD, D/Max-2550 X-ray diffractometer with Cu K $\alpha$  irradiation) at a grazing angle of 4°. The surface and cross-section morphologies of the coatings were characterized by a scanning electron microscope (SEM, Hitachi S-4800, equipped with GENEIS 4000 energy dispersive X-ray (EDX) analysis detector). The surface images were taken by an atomic force microscopy (AFM, NanosurfNaio AFM) in a contact mode. The microstructure was further observed with a transmission electron microscopy (TEM, FEI Tecnai G2F20). Thin foils for TEM analysis were prepared using the focused ion beam technique (FIB, FEI Quanta 3D FEG), together with the OminiProbe in-situ lift out system. The atomic bonding ordering of the coatings was analyzed by a Raman spectroscopy (LABRAM,HR-800) in the excitation line of 514.5 nm.

The contact angle (CA) with deionized water was carried out by a contact angel meter (SL200B, Solon Tech., Shanghai) based on a sessile drop measuring method with a water droplet volume of 4 µL. The tests were conducted within 10 min after the samples were prepared. Tests of six different locations on each sample were taken to ensure homogeneity. The hardness and elastic modulus of the coatings and the Ti6Al4V substrate were obtained by a nanoindentor (Agilent technologies, G-200) with a Berkovich diamond indenter and calculated by Oliver-Pharr method. The indentation depth was 100 nm, which was < 10% of the coating thickness to minimize the substrate effects. The internal stress of the films was calculated using Stoney's equation. The curvature was estimated by measuring 10 mm profiles on films deposited over silicon substrates using a Bruker Dektak profilometer. The biotribological tests were carried out by a ball-on-disk tribometer in FBS at a sliding speed was  $0.1 \text{ m s}^{-1}$ .  $Si_3N_4$  ceramic balls (4 mm in diameter, hardness in 1500 HV) were set as the counterpart at applied loads of 2 N and 10 N. In addition, the multilayer was also tested at a load of 2 N for 24 h (sliding distance of 8.64 km) in order to evaluate the long-term tribological performance. The wear rate of the coatings was defined as volume loss per sliding distance, calculated by measuring the wear tracks.

The corrosion tests were performed on a CHI-660E electrochemical workshop in simulated body fluid (Hank's solution) with a platinum plate as the counter electrode, and a saturated calomel electrode as the reference electrode. The composition of Hank's solution is listed in Table 1. Before the tests, all the samples were immersed in Hank's solution for 2 h. The open circuit potential (OCP) was registered for 1 h. Subsequently, the potentiodynamic polarization tests were carried out at a scan rate of 0.167 mV s $^{-1}$ .

**Table 1**The composition of the Hank's solution.

Component	Concentration (g $L^{-1}$ )	Purity (%)
NaCl	8.0	≥99.5
KCl	0.4	≥99.5
CaCl <sub>2</sub>	0.14	≥96.0
NaHCO <sub>3</sub>	0.35	≥99.5
$MgCl_2 \cdot 6H_2O$	0.1	≥98.0
$Na_2HPO_4 \cdot 2H_2O$	0.06	≥99.0
KH <sub>2</sub> PO <sub>4</sub>	0.06	≥99.5
$MgSO_4 \cdot 7H_2O$	0.06	≥99.0

#### 3. Results and discussion

Fig. 1 shows the XRD pattern ZrN/Zr/a-C multilayer. The diffraction peaks can be indexed with ZrN (fm3m) and Zr (P63/mmc). The broad peaks indicate that the grain sizes of ZrN and Zr are small. Fig. 2 presents the surface and cross-section SEM images of these coatings. The ZrN coating shows a distinct columnar structure (Fig. 2a), while the a-C coating exhibits a fine and unobvious columnar structure (Fig. 2c). The ZrN/Zr/a-C coating contains a Zr interlayer and multilayers (Fig. 2e). It is worth noting that for the ZrN/Zr/a-C multilayer, although the columnar structure of Zr interlayer can be identified, the columnar characteristics is not distinct in the multilayered part, which is benefit for mechanical and corrosion performance. It can be seen the presence of holes on the surface of ZrN coating (Fig. 2b), while the a-C coating and ZrN/Zr/a-C multilayer present relatively dense surface (Fig. 2d, f).

In order to further understand the surface morphology of the ZrN/Zr/a-C multilayer, typical AFM surface images of the coatings are shown in Fig. 3. It can be seen that all the coatings exhibits relatively smooth granular structure. The root mean square roughness ( $R_{\rm q}$ ) of ZrN, a-C and ZrN/Zr/a-C multilayer coatings is about 6.3, 2.7 and 6.6 nm respectively. The low surface roughness of these coatings may benefit their tribological properties.

Fig. 4 presents the microstructure of the ZrN/Zr/a-C multilayer in detail. The coating is composed of a Zr interlayer and the multilayers (Fig. 4a), which is in accordance with the SEM analysis. It can be seen that the multilayered architecture consists of well separated a-C layers and ZrN/Zr layers. In addition, it can be seen that the roughness is additive from bottom to top. The nanostructure of ZrN/Zr layers is further presented in Fig. 4b and c. The Zr layers are between the a-C and ZrN layers. The Zr layers are composed of lots metallic Zr nanocrystallites with hcp structure, while the ZrN layers consist of a large amount of fcc ZrN nanocrystallites, which correspond well with the XRD pattern. The nanostructure results from the deposition process. After depositing the a-C layer, the Zr layer was deposited in an argon atmosphere by

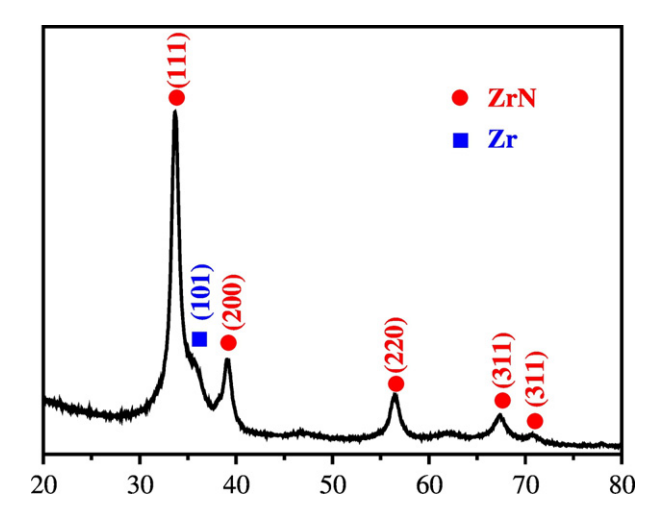


Fig. 1. XRD pattern of ZrN/Zr/a-C multilayer.

# Download English Version:

# https://daneshyari.com/en/article/5465111

Download Persian Version:

https://daneshyari.com/article/5465111

<u>Daneshyari.com</u>